Molecular Science

AIMS Molecular Science, 3(3): 338-356.
DOI: 10.3934/molsci.2016.3.338
Received 22 May 2016,
Accepted 13 July 2016,
Published 15 July 2016

http://www.aimspress.com/journal/Molecular

Review

Application of fluorescently labelled lectins for the study of polysaccharides in biofilms with a focus on biofouling of nanofiltration membranes

Mohamed Amine Ben Mlouka, Thomas Cousseau, and Patrick Di Martino*

Laboratoire ERRMECe, Université de Cergy-Pontoise, Cergy-Pontoise, France

* **Correspondence:** Email: Patrick.di-martino@u-cergy.fr; Tel: +33 134256606.

Abstract: The biofilm state is the dominant microbial lifestyle in nature. A biofilm can be defined as cells organised as microcolonies embedded in an organic polymer matrix of microbial origin living at an interface between two different liquids, air and liquid, or solid and liquid. The biofilm matrix is made of extracellular polymeric substances, polysaccharides being considered as the major structural components of the matrix. Fluorescently labelled lectins have been widely used to stain microbial extracellular glycoconjugates in natural and artificial environments, and to study specific bacterial species or highly complex environments. Biofilm development at the membrane surface conducting to biofouling is one of the major problems encountered during drinking water production by filtration. Biofouling affects the durability and effectiveness of filtration membranes. Biofouling can be reduced by pretreatments in order to control two key parameters of water, the bioavailable organic matter concentration and the concentration of live bacteria. Nanofiltration (NF) is a high technology process particularly suited to the treatment of surface waters to produce drinking water that is highly sensitive to biofouling. The development of strategies for fouling prevention and control requires characterizing the fouling material composition and organisation before and after NF membrane cleaning. The aim of this review is to present basics of biofilm analyses after staining with fluorescently labelled lectins and to focus on the use of fluorescent lectins and confocal laser scanning microscopy to analyse NF membrane biofouling.

Keywords: lectin; fluorescence; polysaccharide; matrix; biofilm; nanofiltration; pretreatment; cleaning; drinking water

1. Introduction

In nature, most of the microbial biomass is organised as sessile communities named biofilms. A biofilm can be defined as cells organised as microcolonies embedded in an organic polymer matrix of microbial origin living at an interface between two different liquids, gas and liquid, or solid and liquid, Figure 1 [1–3]. The biofilms at the solid-liquid interface are the most studied type of biofilm. The biofilms at solid-liquid interfaces are the major cause of biofouling and biodeterioration of materials [4,5], and a common cause of persistent infections [6]. Biofilm formation in the human gut by probiotic bacteria can also have beneficial health effects in prevention of diseases [7]. The biofilms at the liquid-liquid interface have been described mainly in aquatic environments. In marine environments, the biofilm formation at liquid-liquid interfaces results from adaptation of microorganisms to degrade insoluble hydrophobic organic compounds such as lipids and hydrocarbons present in water [1,8]. Biofilm formation in droplets of hydrophobic substances such as fuel or oil is involved in biodegradation of pollution [9–11]. The biofilms at the air-liquid interface form-floating structures also named pellicules [12,13]. Biofilms at the air-liquid interface are facing opposite gradients of nutrient and oxygen, with access to abundant nutrients from the solution below and oxygen from the air above [14,15]. The formation of biofilms at the air-liquid interface can require an initial first step of flocculation: during the first hours of growth in broth in static conditions, *Mycobacterium smegmatis* forms isolated flocs and between 18 and 30 hours, the matrix becomes rigid and pellicle forms [16].

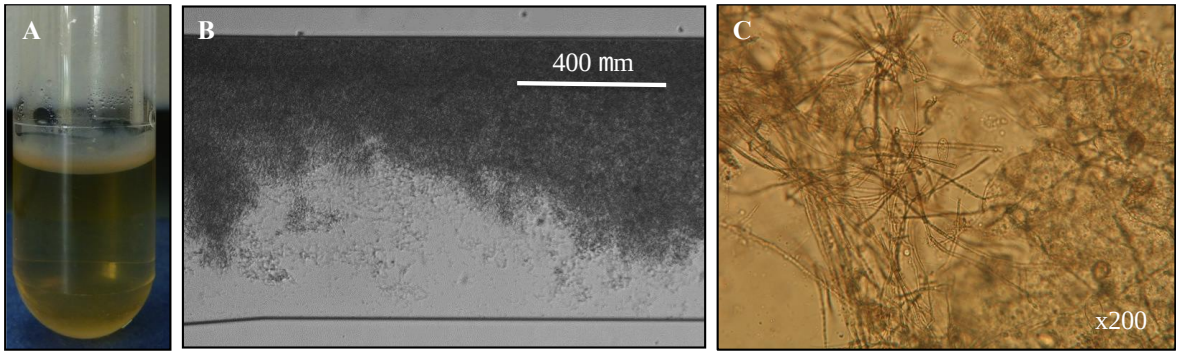

Figure 1. (A) Pellicule formed in static conditions by *Bacillus subtilis* at the interface between air and TS broth after 24 h at 37 °C. (B) Biofilm formed in high flux conditions (1 dyn/cm^2) by *Bacillus subtilis* at the interface solid-liquid in a microfluidic system (BioFlux) after 24 h at 37 °C. (C) Biofilm formed in high pressure filtration tubes in a nanofiltration drinking water production plant.

Irrespective of the location of the biofilm, the matrix is made of extracellular polymeric substances (EPS) comprising polysaccharides, proteins, extracellular DNA, and other substances such as lipids. Extracellular polysaccharides are considered as the major structural components of the matrix [17]. Inside biofilms, matrix constituents and most of microbial cells are invisible but can be observed and characterized after staining with fluorochromes or molecules coupled to fluorochromes. Microbial cells can be stained with fluorescent DNA-binding stains like DAPI, acridine orange, SYBR green, or SYTO 9, polysaccharides can be stained with fluorescent lectins and proteins can be stained with Alexa fluor succinimidyl ester, fluoresceinisothiocyanate isomer I or SYPRO Orange [18–21].

Different biofilm components can be stained simultaneously with different fluorophores. For example, clusters of cells and matrix proteins have been studied among *S. epidermidis* biofilms grown in flow cell conditions [18]; biofilm flocs have been characterized either from drinking water treatment plants [22] or from wastewater treatment plants [20]; biofouling of hollow fibre ultrafiltration membranes has been studied at different operational conditions [22]. Multi-staining approaches can generate peak interference between two channels when the range of emission of two fluorochromes overlap significantly and the excitation level is different between the two [23]. Testing different combinations of fluorophores along with different mounting media, carefully selecting the excitation and emission wavelengths, and using spectral imaging rather than standard channel mode can minimize peak interference [19,24]. Among EPS, extracellular polysaccharides are probably the most studied macromolecules [17]. Fluorescently labelled lectins have been widely used to stain microbial extracellular glycoconjugates in natural and artificial environments, and to study specific bacterial species or highly complex environments. Lectins are proteins obtained from a wide variety of natural sources including seeds, plant roots, plant barks, animal, fungal and bacterial cells. The specificity and affinity of lectins for carbohydrate targets can be compared to those of antigen-antibody interactions [25]. The binding specificities of several lectins used in biofilm research are presented in Table 1.

Table 1. Main lectins used in the analysis of biofilms classified by ligand specificity.

Symbol	Name	Source	Ligand motif	Reference
Mannose Binding Lectins				
AMA	*Arum maculatum* Agglutinin	*Arum maculatum*	Man	[26]
Con A	Concanavalin A	*Canavalia ensiformis*	Branched α-mannosidic structures; high-mannose type, hybrid type and biantennary complex type N-Glycans	[20,24,25,27–42]
CPA	Pure *Cicer arietinum* Lectin	*Cicer arietinum*	Man	[42]
GNA	Snowdrop Lectin	*Galanthus nivalis*	α 1-3 and α 1-6 linked high mannose structures	[35]
HHA, HHL, AL	*Amaryllis* Lectin, *Hippeastrum* Hybrid Lectin	*Hippeastrum Amaryllis*	α-Man	[35]
LCH, LCA	Lentil Lectin	*Lens culinaris*	Fucosylated core region of bi- and triantennary complex type N-Glycans	[41]
PMA	*Polygonatum multiflorum* Agglutinin	*Polygonatum multiflorum*	Mannose Branched	[35,43]
Mannose/Galactose/N-acetylgalactosamine binding Lectins				
DGL	*Dioclea grandiflora* Lectin	*Dioclea grandiflora*	Man, Glc	[35]
LcH	*Lens culinaris* Agglutinin or *Lentil* Lectin	*Lens culinaris*	α-Man, Fucose linked to chitobiose core of oligosaccharide, α-Glc, α-GlcNAc	[26,44]
NI (no information)	*Lathyrus odoratus* Lectin	*Lathyrus odoratus*	α-Man, Glc, GlcNAc	[44]

PSA	*Pisum sativum* Agglutinin	*Pisum sativum*	α-Man, α-Glc, α-GlcNAc	[35,41,43]
Galactose/N-acetylgalactosamine binding Lectins				
ACL, ACA	*Amaranthus caudatus* Lectin	*Amaranthus caudatus*	[gal(β1,3)galNAc, gal(β1,3)Neu5Ac]	[26,42,44]
AIA	*Artocarpus integrifolia* Lectin (Jackfruit)	*Artocarpus integrifolia*	Gal; GalNAc	[35,42]
DBA	Biotinylated *Dolichos biflorus* Agglutinin	*Dolichos biflorus*	α-GalNAc	[26,41,43–45]
ECA, ECL	*Erythrina cristagalli* Agglutinin, Lectin	*Erythrina cristagalli*	Gal, GalNAc, Lac	[42]
GSL, GS-I or BSL	*Griffonia simplicifolia* Lectin or *Bandeiraea simplicifolia* Lectin	*Bandeiraea simplicifolia*	α-D-Gal, N-acetyl-α-D-Gal	[28,35,40–42]
GHA	*Glechoma hederacea*	*Glechoma hederacea Agglutinin*	GalNAc	[42]
HAA	*Helix aspersa* Agglutinin	*Helix aspersa*	GalNAc, GlcNAc	[41,42,44]
HPA	*Helix pomatia* Agglutinin	*Helix pomatia*	α-GalNAc	[26,35,42]
IAA	*Iberis amara* Agglutinin	*Iberis amara*	GlcNAc	[26,33,35]
IRA	*lris hybrid* Lectin	*lris hybrid*	GalNAc	
LEL or LT, LEA	*Lycopersicon Esculentum* Lectin or Tomato Lectin	*Lycopersicon esculentum*	GlcNAc(β1,4), GlcNAc oligomers	[26,35,42,44,46,47]
PNA	Peanut Agglutinin	*Arachis hypogaea*	Galβ1-3GalNAcα1-Ser/Thr (T-Antigen)	[26,28,31,32,36,39–42,44,46–50]
MOA	*Marasmius oreades* Agglutinin	*Marasmius oreades*	α 1-3-Gal homopolymers, α-1-3-Gal-β-1-4-GlcNAc heteropolymers	[42,43]
MPL, MPA	*Maclura Pomifera* Lectin	*Maclura pomifera*	[α-Gal, α-GalNAc, Gal(β1,3)GalNAc]	[35,44]
MNA-G	*Morniga G* Lectin	*Morniga G*	Gal	[35]
PHA	*Phaseolus vulgaris* Agglutinin	*Phaseolus vulgaris*	GalNAc	[31,35,36,41,44,48]
PA-I	*Pseudomonas aeruginosa*	*Pseudomonas aeruginosa*	D-Gal	[26,33,35,48]
RCA	*Ricinus communis* Agglutinin	*Ricinus communis (Castor Bean)*	Glc, GalNAc	[41]
RTA	*Trifolium repens* Lectin	*Trifolium repens*	2-deoxyglucose	[44]
SBA	Soybean Agglutinin Lectin (Glycine max)	*Soybean*	α-GalNAc, β-GalNAc	[26,32,41]
SJA	*Sophora japonica* Agglutinin	*Sophora japonica*	GalNAc	[35,41]
STA	*Solanum tuberosum* Agglutinin	*Solanum tuberosum*	GluNAc	[35]
SVAM	Snake Venom Agglutinin	*Naja mossambica*	α or βGalNAc	[51]

VRA	*Vigna radiata* Aglutinin	*Vigna radiata*	α-Gal	[43]
VVA	*Vicia villosa* Agglutinin	*Vicia villosa*	α-GalNAc	[26,35]
WFA	*Wisteria floribunda* Lectin	*Wisteria floribunda*	[terminal GalNAc(β1,4), terminal GalNAc(β1,3) terminal GalNAc(α1,3)]	[35,42,44,52]
WGA, VGA	Wheat Germ Agglutinin	*Triticum vulgaris*	GlcNAcβ1-4GlcNAcβ1-4GlcNAc, Neu5Ac(sialic acid)	[25,26,28,30,34,36,39–43,45,46,48–50]
Sialic acid/N-acetylglucosamine binding Lectins				
CCA	Crude *Cancer antennarius*	*Cancer antennarius*	9-O-Ac-NeuAc, 4-O-Ac-NeuAc	[43]
HMA	*Homarus americanus* Agglutinin	*Homarus americanus*	Sialic acid, N-Acetylneuraminic acid, N-Glycolyneuraminic acid	[26,33,42]
LFA	*Limax flavus* Lectin	*Limax flavus*	Sialic acid	[42]
Limulin	*Horseshoe crab*	*Limulus polyphemus*	N-acetylneuraminic acid D-glucuronic acid	[28,35,48]
MAL, MAA	*Maackia amurensis* Lectin	*Maackia amurensis*	Neu5Ac/Glc, α2-3Galβ1-4GlcNAcβ1-R	[43]
Fucose/Galactose/N-acetylgalactosamine binding Lectins				
ECorA	*Erythrina corallodendron* Agglutinin	*Erythrina corallodendron*	Fuc-LacNAc, GalNAc, Gal, Lac	[26,43]
LBA	*Lima Bean* Agglutinin	*Phaseolus Lunatus*	{GalNAc(α1,3) [L-fuc(α1,2)Gal], GalNAc}	[44]
Fucose binding Lectins				
AAL	*Aleuria aurantia* Lectin	*Aleuria aurantia*	Fucα1-2Galβ1-4 (Fucα1-3/4)Galβ1-4GlcNAc; R2-GlcNAcβ1-4 (Fucα1-6) GlcNAc-R1	[26,33,35,42,43,53]
UEA-I	*Ulex europaeus* Agglutinin	*Ulex europaeus*	Fuc, Fucα1-2Gal-R	[28,32,33,36,41,46]
LTL	*Lotus tetragonolobus* Lectin	*Lotus tetragonolobus or Tetragonolobus purpureas*	Fuc-α-1-2-Gal-β-1-4-[Fuc(α 1)]-GlcNAc	[28,31,43]
Lectin with no indication of binding specificity				
RPb	*Robinia pseudoacacia* Bark	*Robinia pseudoacacia*	Not Indicated	[44]

Fluorescent lectins have been used successfully to characterize mono-specific biofilms of very different bacteria like *Staphylococcus epidermidis* [54], *Pseudomonas aeruginosa* [34], *Escherichia coli* [55], *Campylobacter jejuni* [42], fresh water diatoms from epilithic biofilms [56], and also highly complex biofilms grown in natural or artificial environments [28,30,32,35,40,43,57]. An example of a highly complex biofilm formed on nanofiltration (NF) membranes during drinking water production is presented in Figure 2. Peanut agglutinin and Wheat germ agglutinin bind efficiently to extracellular substances of the NF biofilm matrix.

Concanavalin A (ConA) was shown to bind to levan, a major exopolysaccharide produced by *P. syringae* [51]. ConA binding in mature biofilms suggested that levan might accumulate within cell-depleted voids in the centre of microcolonies and in blebs [51]. UEA was shown to bind to a

fucose-containing exopolysaccharide present in “dome” structures observed under flow conditions in *Burkholderia thailandensis* biofilms [41]. Different lectins have been shown to have different binding patterns inside microcolonies and/or biofilms: Among biofilms formed from the south Saskatchewan river, *Triticum vulgaris* and *Canavalia ensiformis* lectins bind to cell surfaces and/or to cell associated polysaccharides, *Tetragonolobus purpureas* binds to polysaccharides in the bulk of the structure, *Arachis hypogea* and *Solanum tulerosum* lectins bind to polysaccharides in the outer layer of the structure [58]. In order to stain a large part of extracellular polysaccharides in a biofilm, it is recommended to use cocktails of lectins. Nevertheless, since many lectins are glycoproteins, some lectins recognize each other; therefore possible mixtures have to be tested pairwise for precipitation before they can be used inside a cocktail. EPS of a single microcolony can be stained by at least one and up to four different lectins, each recognizing unique glycoconjugates in the microbial aggregate [58].

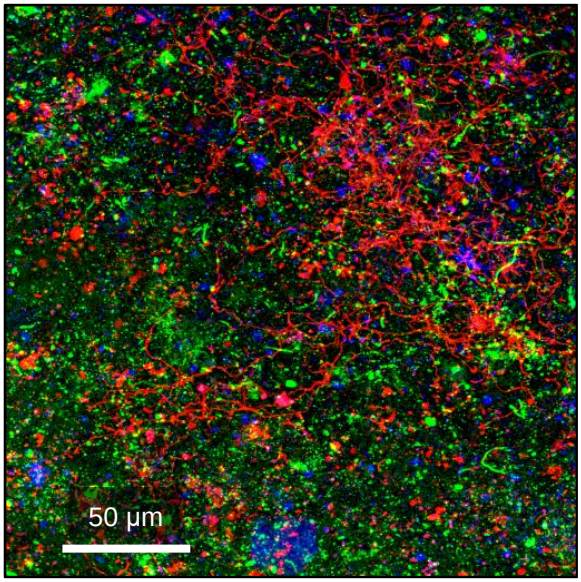

Figure 2. Confocal laser scanning microscopy observations of the microbial and exopolysacharide components of a biofilm formed on a nanofiltration membrane during drinking water production. In blue, the microbial microcolonies are stained with DAPI. In red, extracellular polysaccharides are stained with the peanut agglutinin-TRITC lectin. In green, extracellular polysaccharides are stained with the wheat germ agglutinin-FITC lectin.

The “fluorescence lectin-binding analysis” can be used in combination with fluorescent in situ hybridization to correlate lectin binding with cell identification [26,42,44,48,58]. This combined method was efficient to visualize glycoconjugate components of the EPS on the single cell level inside aggregates and flocs for both procaryotic and eukaryotic cells [48]. Indeed, lectins from *A. hypogaea*, *P. aeruginosa*, and *P. vulgaris* stained distinct glycoconjugates originating from different eukaryotic and prokaryotic microorganisms inside lotic microbial aggregates from the Elbe river [48].

The use of fluorescent lectins is a powerful approach for qualitative and quantitative characterization of biofilms. Parts 2 and 3 are focused onto the use of fluorescent lectins to study biofouling of nanofiltration membranes in a context of drinking water production. Parts 2 and 3 constitute detailed illustrations of this particular application of fluorescent lectins that can be extrapolated to many other biofilm formation contexts.

2. Use of lectins to assess membrane biofouling during drinking water production

Drinking water requires high quality because it must meet the needs of human bodies and the corresponding requirements of hygiene and health. The definition of a drinking water is governed by standards that set maximum content limits for certain harmful substances that may be present in the water. Guidelines for Drinking-water Quality edited by the World Health Organization (WHO) are used as the scientific basis for standard setting in most countries [59]. A drinking water must be free of pathogens such as viruses or bacteria, and parasitic organisms. It must not contain certain minerals considered toxic, such as nitrates, phosphates and heavy metals, organic compounds such as hydrocarbons and pesticides. Conversely, the presence of certain substances, such as trace elements may be highly desired because regarded as essential to the human body. In this context, the treatment to clean water and make it drinkable is a major economic and health issue.

Filtration at the nanometer scale, i.e. Nanofiltration (NF), is a high technology process particularly suited to the treatment of surface waters to produce drinking water [60]. Indeed, NF provides a barrier to eliminate viruses, bacteria and parasites but also micro-pollutants such as pesticides and drug residues and therefore to obtain a water of great microbiological and chemical purity [61]. NF membranes are costly and their effectiveness and durability are limited by fouling [62]. Membrane fouling is a highly complex phenomenon caused by dissolved inorganic and organic components, inert colloids, and microorganisms. Fouling means accumulation of matter on the membrane surface and decrease of filtration performance. Biofouling seems to play a major role in NF membranes fouling during drinking water production [63,64]. Biofouling is a term used to describe all instances of fouling where biologically active organisms are involved [65].

The development of strategies for fouling prevention and control requires characterizing the fouling material composition and organisation [66,67]. The use of fluorescence microscopy associated with fluorescently labelled lectins and a DNA-specific fluorescent stain like DAPI (4’,6-diamidino-2-phenyindole dihydrochloride) has been evaluated to characterize NF membrane foulants in the drinking water plant of Méry sur Oise, France [40]. Double staining with two lectins, one FITC- and one TRITC-labelled were done with a mixture of *Bandeiraea simplicifolia* agglutinin (BS-1) and concanavalin A (ConA) or a mixture of peanut agglutinin (PNA) and wheat germ agglutinin (WGA). Membranes in service for at least 5 years were autopsied after extraction of filtration modules from the plant. To determine the seasonal variations of the foulants, membrane autopsies and analyses were done in March, June and September. Since the biofouling matter contains living microorganisms and active exoenzymes, it is essential to realize a fixation with paraformaldehyde as fast as possible after the membrane autopsy to avoid detachment, growth or autodigestion of the biomass. Extensive washing with filter-sterilized (0.2 μm) water is needed after fixation to remove paraformaldehyde in order to avoid not specific fixation of lectins during staining experiments. The NF200 B-400 membranes used in the plant contain an ultra-thin polypiperazine top layer (DOW, La Plaine Saint Denis, France). The NF200 B-400 membranes have a low molecular weight cut-off, high negative charge, and low hydrophobicity to efficiently remove hydrophobic natural organic matter through electrostatic repulsion/size exclusion [68]. Autofluorescence emission by polymer contents of filtration membranes can be observed after excitation at the wavelengths used in histology, Figure 3. The background level of fluorescence from polymers depends on their content in aromatic structures and conjugated double bonds in their molecular structure [69].

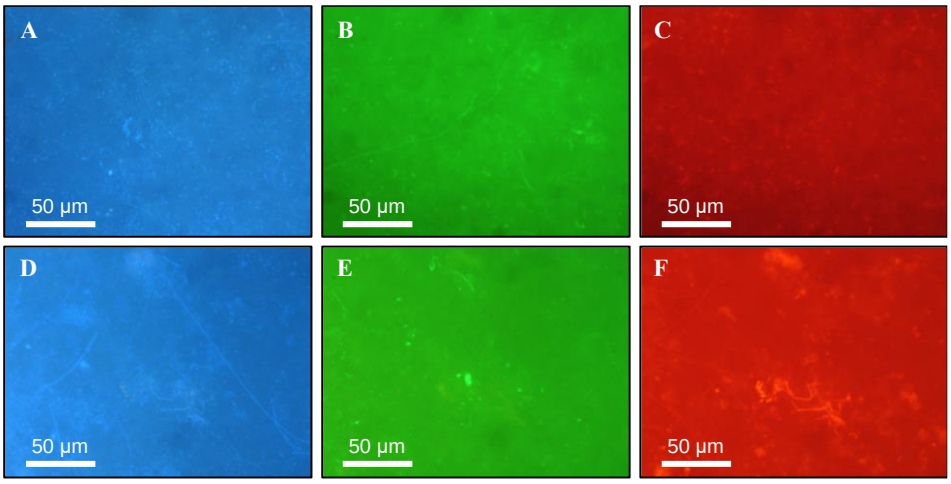

Figure 3. Interactions between fluorescently labelled lectins and fouled membranes, as visualized by epifluorescence microscopy. Shown are fouled membranes extracted in March [(A) to (C)], and September [(D) to (F)], stained with: DAPI + peanut agglutinin-TRITC + wheat germ agglutinin-FITC. The panels coloured in blue [(A), (D)], green [(B), (E)] and red [(C), (F)] correspond to observations after illumination at 364, 494, and 540 nm respectively.

As shown in Figure 3, the background level of autofluorescence of the filtration membranes was easily observable but did not prevent observing the fluorescence emission by stained microbial cells and natural exopolymers. Epifluorescence observations after DAPI excitation at 364 nm showed the presence of many bacterial microcolonies interspersed at the membrane surface. The DAPI staining increased from March to September indicating that bacterial accumulation occurred at the membrane surface. Epifluorescence observations after FITC excitation at 494 nm, and TRITC excitation at 550 nm revealed the presence of polymeric carbohydrate structures located on cell surfaces and polymeric carbohydrate structures located extracellularly throughout the foulants matrix. Lectin staining was not only concentrated in areas where microcolonies were present but also extended in areas devoid of microbial cells. This binding pattern of the lectins has been previously observed with biofilms grown in vitro with river water as the sole source of microorganisms and nutrients [28]. Lectin staining increased from March to September, showing that the increase in sessile bacteria was associated with an increase in EPS production indicating biofilm accumulation. The polysaccharide composition of the fouling layer changed with time certainly as a consequence of qualitative and quantitative modifications among the populations of sessile cells. Such an analysis by epifluorescence microscopy after labelling with DAPI and fluorescent lectins is an approach that can be implemented by an industrial laboratory in a production plant. The equipment and reagents are not very expensive but it is necessary to have qualified technical personnel trained specifically. Confocal laser scanning microscopy was used to study the spatial organization and distribution of the fouling layer at the membrane surface of the same samples. Examples of these observations are shown in Figure 4.

The post-acquisition Leica Confocal Software allowed the elimination of the membrane autofluorescence background. CLSM analysis confirmed that most of the stained polysaccharides were located extracellularly throughout the biofilm matrix. A high degree of spatial organization and high heterogeneity were observed within the fouling material. Depending on the lectin, stained EPS

were shown as long and entangled fibres, short fibres and cloud stained areas. The dominant lectin binding was with BS-1 revealing high occurrence of galactosides residues in the polysaccharide part of the foulants. The microbial cells, mainly organized as microcolonies interspersed at the membrane surface, were localized in the superficial layer of the fouling deposit. These staining patterns suggested that the fouling layer was organized as an interpenetrated network mainly composed of exopolysaccharides supporting microbial cells adhesion and growth. The more sophisticated and expensive CLSM gave the opportunity to observe the spatial organization and 3D structure of the foulants. The fouling material exhibited the same characteristics as a biofilm. These biofilms developed at the surface of membranes in a drinking water plant may result from the presence of microbial cells and nutrients coming from feed water and also from material that has not been removed even after successive cleaning and production processes. The CLSM analysis after labelling with DAPI and fluorescent lectins is an approach that cannot be implemented by an industrial laboratory in a production plant. The equipment is very expensive and the handling of the microscope is quite complex. However, this approach can be outsourced to a specialized laboratory or analytical platform. Indeed, the realization of samples and their stabilization by treatment with paraformaldehyde are quite feasible on site, the fixed samples can then be sent to an analytical laboratory, which will perform staining and microscope observations.

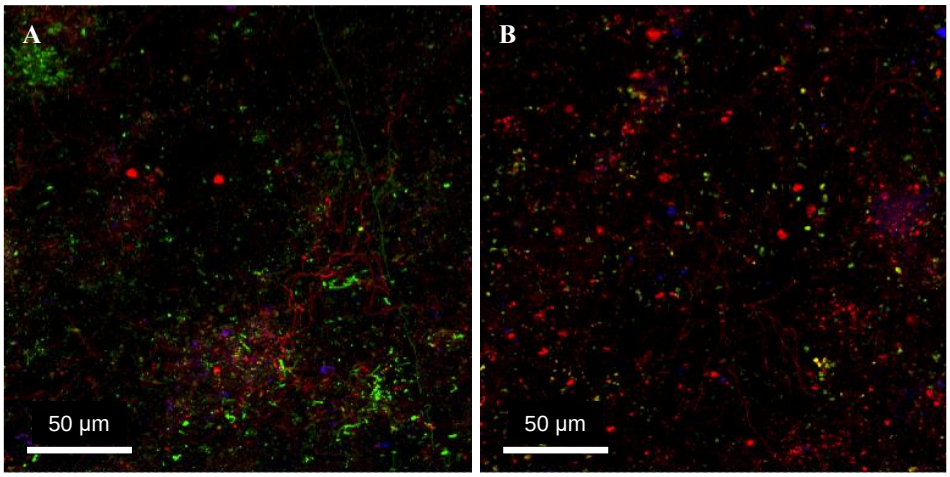

Figure 4. Interactions between fluorescently labelled lectins and fouled membranes, as visualized by confocal laser scanning microscopy. Shown are fouled membranes extracted in September, stained with: DAPI + peanut agglutinin-TRITC + wheat germ agglutinin-FITC [A] and DAPI + BS-1-TRITC + Concanavalin A-FITC [B].

The accumulation of microorganisms on the membrane surface called biofouling results from microbial deposition and growth on the membrane [63]. During NF operation, biofilm development is made easier by bacterial trapping and nutrient concentration at the membrane surface during filtration. The development of strategies for fouling prevention and control also requires characterizing the kinetic development of biofouling [66,67]. The fluorescence lectin-binding analysis has been used to characterize the kinetic development of biofilm for two years on NF membranes at the Méry-sur-Oise plant, France [49]: the biofilm thickness, architecture and abundance were studied after CLSM and computer analyses and membrane performance was recorded over time. The membrane surface coverage rate by the biofilm was determined after

conversion of colour images acquired by CLSM observation to black and white. The percentage of the area covered by the biofilm was obtained by calculating the ratio between the black and white pixels. Biofilm thickness was determined by multiplying the number of slices collected by the thickness of each slice as previously described [70]. The growth in thickness of the biofilm was greater during the first 80 days of filtration, Figure 5.

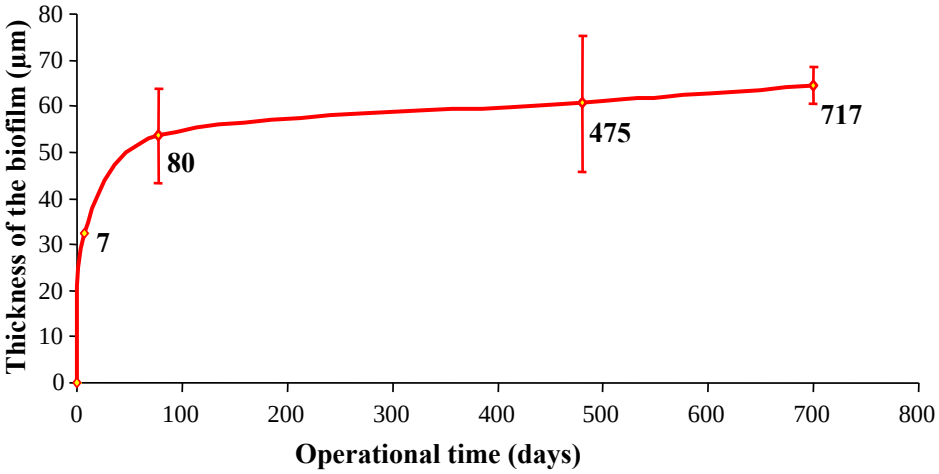

Figure 5. Quantitative evolution of the biofouling layer thickness by confocal laser scanning microscopy after lectin staining. The values are means of five independent measurements ± standard deviation.

At the end of the incubation time, after 717 days, the maximum biofilm thickness was 64 ± 4 µm. A NF biofilm thickness of 20–80 µm has been also measured by confocal microscopy imaging using a pilot system fed conventionally treated Ohio River water for 15 months [62]. In this study, confocal microscopy analyses were obtained after staining the biofilm with Baclight bacterial viability kit (Molecular Probes, Inc, Eugene, OR). Thus, only the cellular part of the biofilm corresponding to viable and nonviable bacteria was taken into account. For greater thicknesses, other measurement approaches such as optical coherence tomography can be used [71]. Using this technology, penetration depths up to 1.7 mm can be observed for biofilms. Thicknesses of about 200 µm have been measured for biofilms developed on ultrafiltration membranes during gravity driven membrane filtration of water for around 50 days [71]. Three stages of biofilm growth on NF membranes were discriminated at the Méry-sur-Oise plant, Figure 6: (1) presence of relatively small sessile microcolonies embedded in an EPS matrix (after filtration for seven days); (2) microcolony growth in three dimensions but partial coverage of the membrane (filtration for up to 80 days) and (3) total coverage of the membrane and biofilm maturation by densification (filtration for 80–717 days). Blue stained cells are easily visible at day 80 and day 475 but hardly visible at day 7 and day 717. At day 7, the microcolonies are not large enough to be easily observed, and at D717, the EPS matrix masks most of the cells. The EPS content increased not linearly in the NF biofilms during the incubation period. The concomitant use of PNA and WGA lectins recognizing different saccharide residues showed that there was a modification in the lectin-staining pattern during biofilm maturation. After filtration for 475 days, there were markedly less WGA-stained carbohydrates than PNA stained polysaccharides, whilst after 717 days, the residues stained with one or the other lectin were present in similar proportions. A shift in polysaccharide composition has been previously shown during growth of mono-specific bacterial biofilms [25]. For

Staphylococcus sciuri and *Stenotrophomonas maltophilia*, the increase in EPS production over time was different between saccharides recognized by WGA and sugars binding to concanavalin A. Thus, for different kind of biofilms, the proportions of different polysaccharides in the biofilm matrix can vary depending on the bacterial composition and the stage of maturity.

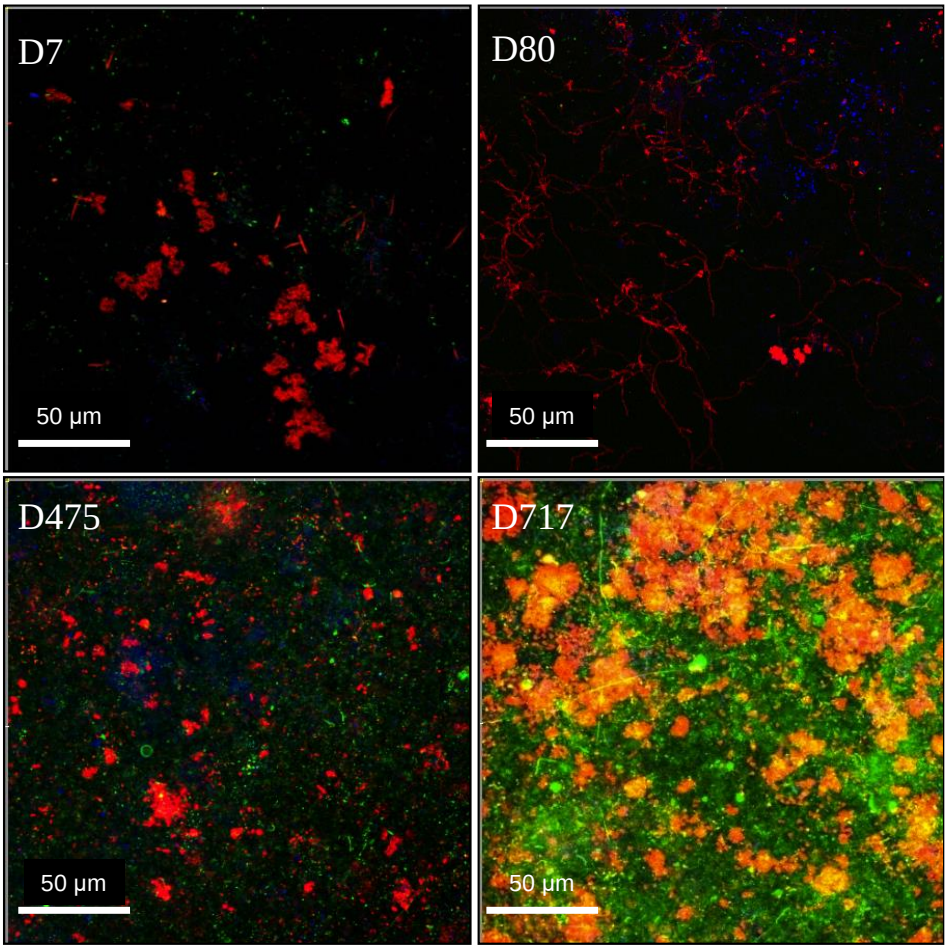

Figure 6. CLSM observations of microbial and exopolysaccharides components of the NF biofilm after 7, 80, 475 and 717 days of operating. In blue, the microbial microcolonies are stained with DAPI. In red, extracellular polysaccharides are stained with the peanut agglutinin-TRITC lectin. In green, extracellular polysaccharides are stained with the wheat germ agglutinin-FITC lectin.

Over time, the development of biofilm on the NF membranes affected the filtration performance. Permeability was affected precociously and continuously during the experiment. The longitudinal pressure drop began to be affected from 200 days of filtration, and increased strongly after filtration for 475 days, a stage where a denser biofilm layer covering most of the membrane surface was formed. This is consistent with the previous observation that the longitudinal pressure drop can be increased by biofouling [72]. Biofilm becomes an issue only when it reaches thickness and surface coverage that cause declined flux and/or increase in pressure drops during NF operation [49,63,73].

3. Use of lectins to assess prevention and control procedures of NF membrane fouling

Coagulation, flocculation, settling and filtration are conventional pre-treatments upstream from NF membranes [74]. To reduce membrane biofouling, the two critical water parameters to control are the bioavailable organic matter concentration and the concentration of live bacteria. The fluorescence lectin-binding analysis was used to compare biofoulants on the surface of membranes operated in identical nanofiltration pilot units fed in parallel with the same water that has undergone different pretreatments: sand filtration (SF) with or without ozonation and granular activated carbon (GAC) adsorption (SF versus SF + GAC) or ozonation and GAC adsorption with or without UV irradiation (400 J/m^2 dose) (SF + GAC versus SF + GAC + UV) [50,74].

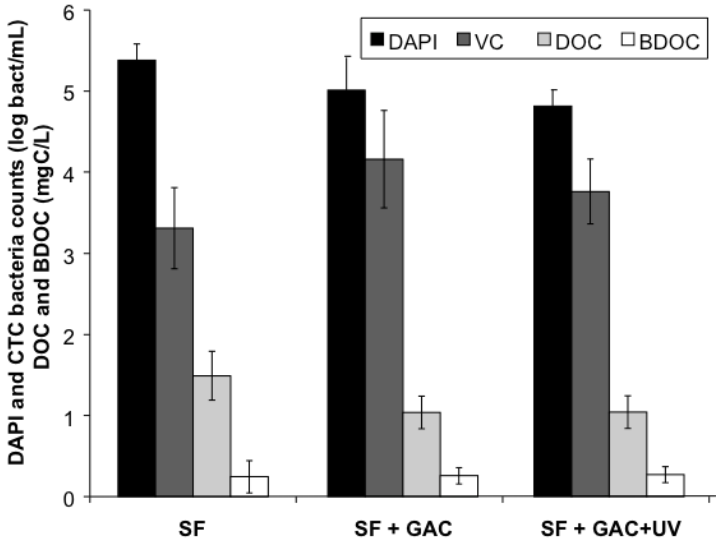

Figure 7. Water quality parameters after different pretreatments. SF, sand filtration. GAC, ozonation and granular activated carbon adsorption. UV, ultraviolet irradiation. TDC, total direct count of bacterial cells by epifluorescence observation after DAPI staining. VC, viable count of bacterial cells after cyano 2-3 dytolyl tetrazolium chloride staining. DOC, concentration in dissolved organic carbon. BDOC, concentration in biodegradable dissolved organic carbon. The values are means of five independent measurements ± standard deviation.

The bioavailable dissolved organic carbon (BDOC) concentration was approximately decreased by a factor 2 after the ozonation and GAC adsorption pretreatment in comparison with the sand filtration pretreatment alone, Figure 7. The viable and total bacterial counts in fed waters were not different between the two conditions. The slight differences observed were not significant. The germicide effect of UV pre-treatment was observed to range between 0.3 and 0.4 log removal of viable bacteria. For all the different feed water quality conditions, the analysis of the foulant matter after DAPI and lectin staining revealed the presence of many microorganisms organized as microcolonies embedded in exopolysaccharides, with a highly heterogeneous repartition, Figure 8. Some areas of the membrane surface were covered by significant amounts of microorganisms and polysaccharides, while others were still virgin and did not present any microbial cells. For all the pretreatments except for UV irradiation, the most intense lectin-binding signals corresponded to the

PNA lectin revealing high occurrence of galactosides residues among foulants. High occurence of galactoside residues seems to be a constant characteristic of exopolysaccharides of the matrix of biofilms fed by river water [28,40]. After UV pretreatment, the most intense signal corresponded to *Lycopersicon esculentum* agglutinin (LEA) binding. This shift in the lectin binding pattern could be related to modifications of the biodiversity among sessile bacteria after UV irradiation: lots of filamentous bacteria were observed on the membrane without UV pretreatment, while they were scarcer on the membrane after UV irradiation [75]. CLSM observations of the foulant deposit demonstrated that the delivery of decreased amounts of nutrients or of decreased amount of live bacteria was associated with a decrease in biofilm development of the NF membranes [50,75]. This decrease in biofilm development was associated with a stabilization of the pressure drop on mid-term duration (several months).

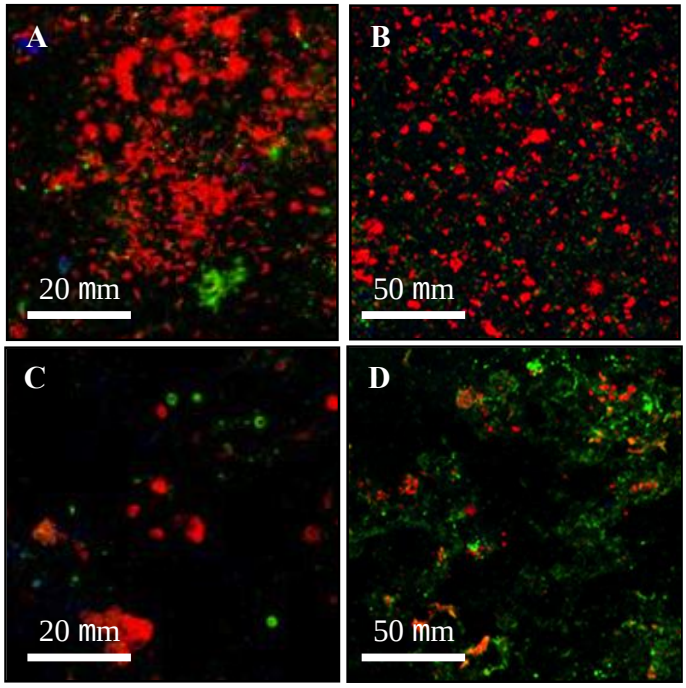

Figure 8. CLSM observations of NF biofilms formed in pilot units fed in parallel with the same water that has undergone different pretreatments: sand filtration (A), sand filtration with ozonation and granular activated carbon (B and C), sand filtration with ozonation and granular activated carbon and UV irradiation (D). Microbial cells are stained with DAPI. Extracellular polysaccharides are stained with the peanut agglutinin-TRITC lectin (A, B, C) and the wheat germ agglutinin-FITC lectin (C), or *Lycopersicon esculentum* agglutinin-FITC (D).

Effective raw water pre-treatment prior to NF is essential to reduce fouling but can't completely avoid the phenomenon. Thus, chemical cleaning is an essential step in maintaining the performance of the filtration process [64,76]. Flux recovery data are usually employed to assess the efficiency of industrial cleaning procedures but does not give any information about foulants removal from the membrane surface. The fluorescence lectin-binding analysis can give complimentary information by comparing biofoulants before and after chemical cleaning and thus can help to improve cleaning procedures. This approach applied to the cleaning in place procedures at the Méry sur Oise drinking

water production plant showed that the organic fouling deposit characteristic of a microbial biofilm was only partially removed after treatment [39]. After cleaning, CLSM observations showed a general decrease of the lectin-staining pattern with differences between lectins: the decrease in lectin staining was high for some lectins (BS-1 and WGA) and weak for others (ConA and PNA). This illustrates the importance of using multiple markers with cocktails of lectins. Removal of microbial cells was revealed by the decrease of the DAPI staining. A decrease of the foulant matter thickness measured by CLSM observation was also reported indicating partial removal of the biofouling deposit. The fluorescence lectin-binding analysis is an efficient tool to assess biofouling removal, but multidisciplinary analyses are needed to take into account all the diversity of the foulant matter. Dry weight measurements, total inorganic carbon and adenosine triphosphate content measurements, inductively coupled plasma-atomic emission spectroscopy, attenuated total reflection Fourier transform infrared spectroscopy can give quantitative and/or qualitative information about foulants removal after cleaning [39,64,77,78]. Moreover, the effects of cleaning onto adhesion forces between the foulant and the membrane surface and between the bulk foulant and the fouling layer or more generally onto mechanical parameters of the foulant matter (viscosity, elasticity) can be analysed by atomic force microscopy or cone-plate rheology, respectively [76,77].

4. Conclusion

Biofilms are highly complex biological structures that form universally at wet interfaces in natural and artificial environments. Fluorescent lectins are powerful tools to characterize the extracellular polymeric substances containing sugars in biofilms. By their specificity, the lectin-binding pattern gives information about the polysaccharide content of the matrix. Fluorescent lectins can be used one by one or collection of lectins with a large panel of specificity can be tested. When the repertoire of lectins able to bind efficiently to the sample analysed is determined, it is recommended to use cocktails of lectins in order to stain a large part of extracellular polysaccharides in the biofilm. Fluorescent lectins can be used alone or with other fluorescent molecules targeting different biofilm components, like fluorescent DNA-binding stains for microbial cells, and SYPRO Orange for proteins. After staining, the biofilm samples can be observed by epifluorescence microscopy to obtain qualitative and semi-quantitative information. An industrial laboratory in a production plant or a teaching laboratory can implement this approach. The stained biofilm samples can also be observed by confocal laser scanning microscopy to obtain complimentary information such as the three-dimensional spatial organization and distribution of EPS in the biofilm structure and quantitative information like depth and biovolume. In this way, fluorescent lectins allow to study the kinetic development of a biofilm, the efficiency of different preventive or curative anti-biofilm treatments.

Conflict of interest

The author confirms that this article content has no conflicts of interest.

References

1. Mounier J, Camus A, Mitteau I, et al. (2014) The marine bacterium *Marinobacter hydrocarbonoclasticus SP17* degrades a wide range of lipids and hydrocarbons through the formation of oleolytic biofilms with distinct gene expression profiles. *FEMS Microbiol Ecol* 90: 816–831.
2. Nait Chabane Y, Marti S, Rihouey C, et al. (2014) Characterisation of pellicles formed by *Acinetobacter baumannii* at the air-liquid interface. *PloS One* 9: e111660.
3. Gagnière H, Di Martino P (2004) Effects of antibiotics on Pseudomonas aeruginosa NK125502 and *Pseudomonas fluorescens M*F0 biofilm formation on immobilized fibronectin. *J Chemother Florence Italy* 16: 244–247.
4. Flemming HC, Schaule G (1996) Measures against biofouling. In: Heitz E, Sand W, Flemming H-C, Eds. *Microbially influenced corrosion of materials – scientific and technological aspects*. Springer, Berlin. 121–139.
5. Di Martino P (2016) What About Biofilms on the Surface of Stone Monuments? *Open Conf Proc J* 6: 14–28.
6. Costerton JW, Stewart PS, Greenberg EP (1999) Bacterial biofilms: a common cause of persistent infections. *Science* 284: 1318–1322.
7. Vastano V, Pagano A, Fusco A, et al. (2016) The Lactobacillus plantarum Eno A1 Enolase Is Involved in Immunostimulation of Caco-2 Cells and in Biofilm Development. *Adv Exp Med Biol* 897: 33–44.
8. Klein B, Grossi V, Bouriat P, et al. (2008) Cytoplasmic wax ester accumulation during biofilm-driven substrate assimilation at the alkane--water interface by *Marinobacter hydrocarbonoclasticus S*P17. *Res Microbiol* 159: 137–144.
9. Baldi F, Ivošević N, Minacci A, et al. (1999) Adhesion of *Acinetobacter Venetianu*s to Diesel Fuel Droplets Studied with In Situ Electrochemical and Molecular Probes. *Appl Environ Microbiol* 65: 2041–2048.
10. Macedo AJ, Kuhlicke U, Neu TR, et al. (2005) Three stages of a biofilm community developing at the liquid-liquid interface between polychlorinated biphenyls and water. *Appl Environ Microbiol* 71: 7301–7309.
11. Pepi M, Minacci A, Di Cello F, et al. (2003) Long-term analysis of diesel fuel consumption in a co-culture of *Acinetobacter Venetianus*, *Pseudomonas putida* and *Alcaligenes faecalis*. *Antonie Van Leeuwenhoek* 83: 3–9.
12. Trejo M, Douarche C, Bailleux V, et al. (2013) Elasticity and wrinkled morphology of Bacillus subtilis pellicles. *Proc Natl Acad Sci U S A* 110: 2011–2016
13. Armitano J, Méjean V, Jourlin-Castelli C (2014) Gram-negative bacteria can also form pellicles. *Environ Microbiol Rep* 6: 534–544.
14. Friedman L, Kolter R (2004) Two genetic loci produce distinct carbohydrate-rich structural components of the *Pseudomonas aeruginosa* biofilm matrix. *J Bacteriol* 186: 4457–4465.
15. Koza A, Hallett PD, Moon CD, et al. (2009) Characterization of a novel air-liquid interface biofilm of *Pseudomonas fluorescens SBW25*. *Microbiol Read Engl* 155: 1397–1406.
16. Sochorová Z, Petráčková D, Sitařová B, et al. (2014) Morphological and proteomic analysis of early stage air-liquid interface biofilm formation in *Mycobacterium smegmatis*. *Microbiol Read Engl* 160: 1346–1356.

17. Lembre P, Lorentz C, Di Martino P (2012) Exopolysaccharides of the Biofilm Matrix: A Complex Biophysical World. In: Dr. Desiree Nedra Karunaratne Ed, *The Complex World of Polysaccharides*. InTech.
18. Stewart PS, Rani SA, Gjersing E, et al. (2007) Observations of cell cluster hollowing in *Staphylococcus epidermidis* biofilms. *Lett Appl Microbiol* 44: 454–457.
19. Chen M-Y, Lee D-J, Tay J-H, et al. (2007) Staining of extracellular polymeric substances and cells in bioaggregates. *Appl Microbiol Biotechnol* 75: 467–474.
20. Nosyk O, ter Haseborg E, Metzger U, et al. (2008) A standardized pre-treatment method of biofilm flocs for fluorescence microscopic characterization. *J Microbiol Methods* 75: 449–456.
21. Wagner M, Ivleva NP, Haisch C, et al. (2009) Combined use of confocal laser scanning microscopy (CLSM) and Raman microscopy (RM): investigations on EPS-Matrix. *Water Re*s 43: 63–76.
22. Sun C, Fiksdal L, Hanssen-Bauer A, et al. (2011) Characterization of membrane biofouling at different operating conditions (flux) in drinking water treatment using confocal laser scanning microscopy (CLSM) and image analysis. *J Membr Sci* 382: 194–201.
23. Murray JM (2005) Confocal microscopy, deconvolution, and structured illumination methods. In: Spector DL, Goldman RD, *Basic methods in microscopy*. Cold Spring Harbour Laboratory Press, New York.
24. Baird FJ, Wadsworth MP, Hill JE (2012) Evaluation and optimization of multiple fluorophore analysis of a *Pseudomonas aeruginosa* biofilm. *J Microbiol Methods* 90: 192–196.
25. Leriche V, Sibille P, Carpentier B (2000) Use of an enzyme-linked lectinsorbent assay to monitor the shift in polysaccharide composition in bacterial biofilms. *Appl Environ Microbiol* 66: 1851–1856.
26. Zippel B, Neu TR (2011) Characterization of glycoconjugates of extracellular polymeric substances in tufa-associated biofilms by using fluorescence lectin-binding analysis. *Appl Environ Microbiol* 77: 505–516.
27. Decho AW, Kawaguchi T (1999) Confocal imaging of in situ natural microbial communities and their extracellular polymeric secretions using Nanoplast resin. *Biotechnology* 27: 1246–1252.
28. Neu T, Swerhone GD, Lawrence JR (2001) Assessment of lectin-binding analysis for in situ detection of glycoconjugates in biofilm systems. *Microbiol Read Engl* 147: 299–313.
29. Neu TR, Kuhlicke U, Lawrence JR (2002) Assessment of fluorochromes for two-photon laser scanning microscopy of biofilms. *Appl Environ Microbiol* 68: 901–909.
30. Yang Y, Sreenivasan PK, Subramanyam R, et al. (2006) Multiparameter assessments to determine the effects of sugars and antimicrobials on a polymicrobial oral biofilm. *Appl Environ Microbiol* 72: 6734–6742.
31. Wigglesworth-Cooksey B, Cooksey KE (2005) Use of fluorophore-conjugated lectins to study cell-cell interactions in model marine biofilms. *Appl Environ Microbiol* 71: 428–435.
32. Lawrence JR, Chenier MR, Roy R, et al. (2004) Microscale and molecular assessment of impacts of nickel, nutrients, and oxygen level on structure and function of river biofilm communities. *Appl Environ Microbiol* 70: 4326–4339.
33. Villacorte LO, Ekowati Y, Neu TR, et al. (2015) Characterisation of algal organic matter produced by bloom-forming marine and freshwater algae. *Water Res* 73: 216–230.

34. Strathmann M, Wingender J, Flemming H-C (2002) Application of fluorescently labelled lectins for the visualization and biochemical characterization of polysaccharides in biofilms of *Pseudomonas aeruginosa*. *J Microbiol Methods* 50: 237–248.
35. Zhang RY, Neu TR, Bellenberg S, et al. (2015) Use of lectins to in situ visualize glycoconjugates of extracellular polymeric substances in acidophilic archaeal biofilms. *Microb Biotechnol* 8: 448–461.
36. Johnsen AR, Hausner M, Schnell A, et al. (2000) Evaluation of fluorescently labeled lectins for noninvasive localization of extracellular polymeric substances in Sphingomonas biofilms. *Appl Environ Microbiol* 66: 3487–3491.
37. Wrede C, Heller C, Reitner J, et al. (2008) Correlative light/electron microscopy for the investigation of microbial mats from Black Sea Cold Seeps. *J Microbiol Methods* 73: 85–91.
38. Herzberg M, Elimelech M (2007) Biofouling of reverse osmosis membranes: Role of biofilm-enhanced osmotic pressure. *J Membr Sci* 295: 11–20.
39. Di Martino P, Doumèche B, Galas L, et al. (2007) Assessing chemical cleaning of nanofiltration membranes in a drinking water production plant: a combination of chemical composition analysis and fluorescence microscopy. *Water Sci Technol* 55: 219–225.
40. Doumèche B, Galas L, Vaudry H, et al. (2007) Membrane Foulants Characterization in a Drinking Water Production Unit. *Food Bioprod Process* 85: 42–48.
41. Tseng BS, Majerczyk CD, Passos da Silva D, et al. (2016) Quorum sensing influences *Burkholderia thailandensis* biofilm development and matrix production. *J Bacteriol* in press.
42. Turonova H, Neu TR, Ulbrich P, et al. (2016) The biofilm matrix of *Campylobacter jejuni* determined by fluorescence lectin-binding analysis. *Biofouling* 32: 597–608.
43. Bennke CM, Neu TR, Fuchs BM, et al. (2013) Mapping glycoconjugate-mediated interactions of marine Bacteroidetes with diatoms. *Syst Appl Microbiol* 36: 417–425.
44. Peltola M, Neu TR, Raulio M, et al. (2008) Architecture of *Deinococcus geothermalis* biofilms on glass and steel: a lectin study. *Environ Microbiol* 10: 1752–1759.
45. Neu TR, Woelfl S, Lawrence JR (2004) Three-dimensional differentiation of photo-autotrophic biofilm constituents by multi-channel laser scanning microscopy (single-photon and two-photon excitation). *J Microbiol Methods* 56: 161–172.
46. Houari A, Picard J, Habarou H, et al. (2008) Rheology of biofilms formed at the surface of NF membranes in a drinking water production unit. *Biofouling* 24: 235–240.
47. Harabi A, Bouzerara F (2011) *Fabrication of Tubular Membrane Supports from Low Price Raw Materials, Using Both Centrifugal Casting and/or Extrusion Methods.* INTECH Open Access Publisher, Chapter 13: 253-274
48. Böckelmann U, Manz W, Neu TR, et al. (2002) Investigation of lotic microbial aggregates by a combined technique of fluorescent in situ hybridization and lectin-binding-analysis. *J Microbiol Methods* 49: 75–87.
49. Houari A, Seyer D, Kecili K, et al. (2013) Kinetic development of biofilm on NF membranes at the Méry-sur-Oise plant, France. *Biofouling* 29: 109–118.
50. Marconnet C, Houari A, Galas L, et al. (2009) Biodegradable dissolved organic carbon concentration of feed water and NF membrane biofouling: a pilot train study. *Desalination* 242: 228–235.
51. Laue H, Schenk A, Li H, et al. (2006) Contribution of alginate and levan production to biofilm formation by Pseudomonas syringae. *Microbiol Read Engl* 152: 2909–2918.

52. Jennings LK, Storek KM, Ledvina HE, et al. (2015) Pel is a cationic exopolysaccharide that cross-links extracellular DNA in the *Pseudomonas aeruginosa* biofilm matrix. *Proc Natl Acad Sci U S A* 112: 11353–11358.
53. Staudt C, Horn H, Hempel DC, et al. (2004) Volumetric measurements of bacterial cells and extracellular polymeric substance glycoconjugates in biofilms. *Biotechnol Bioeng* 88: 585–592.
54. Sanford BA, Thomas VL, Mattingly SJ, et al. (1995) Lectin-biotin assay for slime present in in situ biofilm produced by *Staphylococcus epidermidis* using transmission electron microscopy (TEM). *J Ind Microbiol* 15: 156–161.
55. Maeyama R, Mizunoe Y, Anderson JM, et al. (2004) Confocal imaging of biofilm formation process using fluoroprobed *Escherichia c*oli and fluoro-stained exopolysaccharide. *J Biomed Mater Res A* 70: 274–282.
56. Bahulikar RA, Kroth PG (2007) Localization of EPS components secreted by freshwater diatoms using differential staining with fluorophore-conjugated lectins and other fluorochromes. *Eur J Phycol* 42: 199–208.
57. Hao L, Guo Y, Byrne JM, et al. (2016) Binding of heavy metal ions in aggregates of microbial cells, EPS and biogenic iron minerals measured in-situ using metal- and glycoconjugates-specific fluorophores. *Geochim Cosmochim Acta* 180: 66–96.
58. Lawrence JR, Swerhone GDW, Kuhlicke U, et al. (2007) In situ evidence for microdomains in the polymer matrix of bacterial microcolonies. *Can J Microbiol* 53: 450–458.
59. WHO (2011) *Guidelines for drinking-water quality*, 4 ed. World Health Organization, Geneva.
60. Cyna B, Chagneau G, Bablon G, et al. (2002) Two years of nanofiltration at the Méry-sur-Oise plant, France. *Desalination* 147: 69–75.
61. Hilal N, Al-Zoubi H, Darwish NA, et al. (2004) A comprehensive review of nanofiltration membranes: Treatment, pretreatment, modelling, and atomic force microscopy. *Desalination* 170: 281–308.
62. Speth TF, Summers RS, Gusses AM (1998) Nanofiltration Foulants from a Treated Surface Water. *Environ Sci Technol* 32: 3612–3617.
63. Vrouwenvelder HS, van Paassen JAM, Folmer HC, et al. (1998) Biofouling of membranes for drinking water production. *Desalination* 118: 157–166.
64. Liikanen R, Yli-Kuivila J, Laukkanen R (2002) Efficiency of various chemical cleanings for nanofiltration membrane fouled by conventionally-treated surface water. *J Membr Sci* 195: 265–276.
65. Lappin-Scott HM, Costerton JW (1989) Bacterial biofilms and surface fouling. *Biofouling* 1: 323–342.
66. Flemming H-C, Schaule G, Griebe T, et al. (1997) Biofouling—the Achilles heel of membrane processes. *Desalination* 113: 215–225.
67. Violleau D, Essis-Tome H, Habarou H, et al. (2005) Fouling studies of a polyamide nanofiltration membrane by selected natural organic matter: an analytical approach. *Desalination* 173: 223–238.
68. Koyuncu I, Wiesner MR, Bele C, et al. (2006) Bench-scale assessment of pretreatment to reduce fouling of salt-rejecting membranes. *Desalination* 197: 94–105.
69. Shadpour H, Musyimi H, Chen J, et al. (2006) Physiochemical properties of various polymer substrates and their effects on microchip electrophoresis performance. *J Chromatogr A* 1111: 238–251.

70. Ivnitsky H, Katz I, Minz D, et al. (2007) Bacterial community composition and structure of biofilms developing on nanofiltration membranes applied to wastewater treatment. *Water Res* 41: 3924–3935.
71. Derlon N, Grütter A, Brandenberger F, et al. (2016) The composition and compression of biofilms developed on ultrafiltration membranes determine hydraulic biofilm resistance. *Water Res* 102: 63-72
72. Vrouwenvelder JS, Manolarakis SA, van der Hoek JP, et al. (2008) Quantitative biofouling diagnosis in full scale nanofiltration and reverse osmosis installations. *Water Res* 42: 4856–4868.
73. Ridgway H, Flemming HC (1996) Membrane Biofouling, In: *Water Treatment Membrane Processes*. McGraw Hill, New York.
74. Speth TF, Gusses AM, Scott Summers R (2000) Evaluation of nanofiltration pretreatments for flux loss control. *Desalination* 130: 31–44.
75. Marconnet C, Houari A, Seyer D, et al. (2011) Membrane biofouling control by UV irradiation. *Desalination* 276: 75–81.
76. Li Q, Elimelech M (2004) Organic fouling and chemical cleaning of nanofiltration membranes: measurements and mechanisms. *Environ Sci Technol* 38: 4683–4693.
77. Houari A, Seyer D, Couquard F, et al. (2010) Characterization of the biofouling and cleaning efficiency of nanofiltration membranes. *Biofouling* 26: 15–21.
78. Zhu H, Nyström M (1998) Cleaning results characterized by flux, streaming potential and FTIR measurements. *Colloids Surf Physicochem Eng Asp* 138: 309–321.

AIMS Press